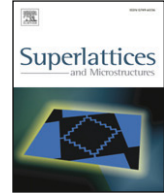




Contents lists available at ScienceDirect

Superlattices and Microstructures

journal homepage: www.elsevier.com/locate/superlattices

DX-center energy calculation with quantitative mobility spectrum analysis in n-AlGaAs/GaAs structures with low Al content

S.B. Lisesivdin^{a,b,*}, H. Altuntas^a, A. Yildiz^c, M. Kasap^a, E. Ozbay^{b,d,e}, S. Ozelik^a

^a Department of Physics, Faculty of Science and Arts, Gazi University, Teknikokullar, 06500 Ankara, Turkey

^b Nanotechnology Research Center, Bilkent University, Bilkent, 06800 Ankara, Turkey

^c Department of Physics, Faculty of Science and Arts, Ahi Evran University, 40100 Kirsehir, Turkey

^d Department of Physics, Bilkent University, Bilkent, 06800 Ankara, Turkey

^e Department of Electrical and Electronics Engineering, Bilkent University, Bilkent, 06800 Ankara, Turkey

ARTICLE INFO

Article history:

Received 12 January 2009

Received in revised form

28 January 2009

Accepted 21 February 2009

Available online 17 March 2009

Keywords:

DX-center

QMSA

AlGaAs/GaAs

Modulation doped

Hall effect

ABSTRACT

Experimental Hall data that were carried out as a function of temperature (60–350 K) and magnetic field (0–1.4 T) were presented for Si-doped low Al content ($x = 0.14$) n-Al_xGa_{1-x}As/GaAs heterostructures that were grown by molecular beam epitaxy (MBE). A 2-dimensional electron gas (2DEG) conduction channel and a bulk conduction channel were founded after implementing quantitative mobility spectrum analysis (QMSA) on the magnetic field dependent Hall data. An important decrease in 2DEG carrier density was observed with increasing temperature. The relationship between the bulk carriers and 2DEG carriers was investigated with 1D self consistent Schrödinger–Poisson simulations. The decrement in the 2DEG carrier density was related to the DX-center carrier trapping. With the simulation data that are not included in the effects of DX-centers, 17 meV of effective barrier height between AlGaAs/GaAs layers was found for high temperatures ($T > 300$ K). With the QMSA extracted values that are influenced by DX-centers, 166 meV of the DX-center activation energy value were founded at the same temperatures.

© 2009 Elsevier Ltd. All rights reserved.

* Corresponding author at: Department of Physics, Faculty of Science and Arts, Gazi University, Teknikokullar, 06500 Ankara, Turkey. Tel.: +90 5412262672.

E-mail address: sblisesivdin@gmail.com (S.B. Lisesivdin).

1. Introduction

Device instabilities such as voltage shift [1], source-drain current transients [2], and hot-electron trapping [3] in n-AlGaAs/GaAs modulation-doped field effect transistors are caused by deep donors or DX-centers [4–6]. The DX centers in bulk semiconductors have been intensively studied for many years especially in the 1980s and 1990s [7–9]. Nonetheless, an investigation of DX-centers and the effects on low dimensional systems are still ongoing processes [10–12].

DX-centers are electron traps that are believed to occur by charge-state-controlled large lattice relaxation [5]. For the n-Al_xGa_{1-x}As/GaAs heterostructures, these centers are shown to exist in S [13], Ge [13], Si [13], Te [14,15], Se [14,16] and Sn [14,17] doped samples grown by all the major growth mechanisms such as molecular beam epitaxy (MBE), liquid phase epitaxy (LPE), or metal organic vapor phase epitaxy (MOVPE) in the composition range of $x > 0.2$. This composition range is highly studied, because two important studies reported two types of donors for the lightly doped n-Al_xGa_{1-x}As/GaAs heterostructures: shallow donors below the composition range $x < 0.2$ and DX-centers above $x > 0.3$ [18,19]. For the highly doped n-AlGaAs, which are essential for high electron mobility transistor application, the importance of DX-centers below the composition range $x < 0.2$ are shown and calculated [3,20].

In this study, we implemented Quantitative Mobility Spectrum Analysis (QMSA) on n-AlGaAs/GaAs semiconductors with no spacer layer. With QMSA, bulk conductivity at n-AlGaAs and the 2-dimensional electron gas (2DEG) conductivity at the n-AlGaAs/GaAs interface is successfully extracted. Without a spacer layer, it is expected that the (2DEG) mobility will be low due to remote impurity scattering [21]. However, not using the spacer layer is essential for this study to investigate the relationship between the carrier densities of the bulk layer and the 2DEG. With the temperature dependent bulk carrier densities and 2DEG densities, the energy of the DX-states are successfully extracted.

2. Experimental techniques

Samples were grown on epi-ready semi-insulating GaAs (100) substrate by molecular beam epitaxy by using a VG-Semicon V80-H solid source MBE system. Samples had an 81.5 nm GaAs layer on substrate and 168.4 nm Si doped n-type Al_{0.14}Ga_{0.86}As layer on the GaAs layer. Layer thicknesses and the Al mole fraction were found with high resolution x-ray diffraction (HRXRD) measurements.

For the resistivity and Hall effect measurements by the van der Pauw method, square shaped ($5 \times 5 \text{ mm}^2$) samples were prepared with four evaporated Au ohmic contacts at the corners. Using gold wires and In soldering, the electrical contacts were made and their ohmic behavior was confirmed with the current–voltage (I – V) characteristics. The measurements were made at 17 temperature steps over a temperature range 60–350 K using a Lake Shore Hall effect measurement system (HMS). At each temperature step the Hall coefficient and resistivity were measured for both current directions, both magnetic field polarization, and all the possible contact configurations at 28 magnetic field steps between 0 and 1.4 T. The magnetic field dependent data were analyzed by using the QMSA technique.

3. Results and discussion

The resistivity and Hall effect measurements of n-Al_{0.14}Ga_{0.86}As/GaAs heterostructures were carried out as a function of temperature (60–350 K) and the magnetic field (0–1.4 T). Fig. 1 shows the temperature dependent Hall mobilities and sheet carrier densities at 0.4 T. Lower mobility at higher temperatures is because of optical phonon scattering limiting. At lower temperatures, mobility is increased with decreasing temperature. These behaviors are typical of 2DEG systems and they are independent of the material system [22]. However, because of the lack of a spacer layer, remote impurities highly scatter the electrons in the quantum well and the mobility decreased drastically. This scattering mechanism is called remote impurity scattering and it is one of the major scattering mechanism at low temperatures [21]. However, in our case, we deliberately did not grow a spacer layer to investigate the relationship between the carriers in the well and the carriers in the AlGaAs

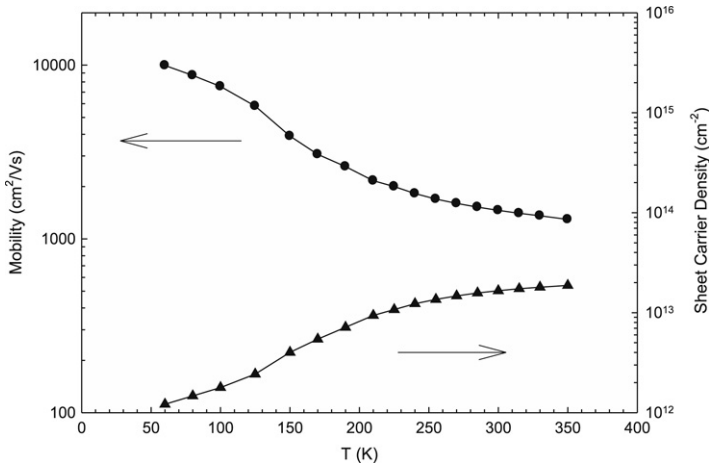


Fig. 1. Temperature dependent Hall mobility and Hall sheet carrier density.

barrier layer. For the measured samples, the Hall sheet carrier density was increased by a factor of 10 with the increasing temperature in the studied temperature range.

Magnetic-field dependent data at each temperature step were analyzed using the QMSA method [23,24]. With the QMSA method, one can easily extract the mobilities and densities of individual electron and holes in bulk semiconductor materials and heterostructures [25,26]. This method is shown to be superior to other methods such as the two-carrier fit, multi carrier fit, and mobility spectrum analysis methods [27–30]. The analysis details are listed in our previous work for AlGaIn/GaN based systems [31]. Fig. 2 shows the Hall results ($B = 0.4$ T) and QMSA results of the n-Al_{0.14}Ga_{0.86}As/GaAs heterostructures as a function of temperature for the mobility and the sheet carrier density. Two carriers are successfully extracted. The one with the higher mobility (blue triangles) shows the 2DEG characteristics. Increased mobility with decreasing temperature and nearly temperature independent carrier density are typical for 2DEG systems [22]. A latter carrier (red squares) is related with a highly doped bulk AlGaAs barrier. The dimensionless product of lowest mobility and the highest field must be greater than unity to clearly identify additional carriers ($\mu_{\min} B_{\max} \geq 1$). For the QMSA studies, $\mu_{\min} B_{\max} = 0.5$ can be recommended as a limit [31]. In this study, this condition seems to be barely fulfilled for the mobilities of the latter carrier extracted by QMSA ($\mu_{\min} B_{\max} \sim 0.3$). However, we also presented successfully extracted different carriers with low mobilities in an AlGaIn/GaN heterostructure grown on sapphire [32]. Because of this barely fulfilled condition, QMSA results of latter carrier are seemed to be scattered. For a carrier with such low product of mobility and magnetic field, results of QMSA represent an important degree of consistency and success which can be attributed to iterative nature of QMSA. It can be easily seen in Fig. 2 (b) that the total carrier density is highly influenced by the bulk carrier. To understand the contributions of these carriers, the conductivities of carriers and the total conductivity are shown in Fig. 3. At high temperatures, bulk carriers supply most of the conductivity. However, bulk carriers are frozen out with the decreasing temperature and the 2DEG conductivity becomes dominant at low temperatures.

As was mentioned above, the temperature independent carrier density is typical of 2DEG systems. In many studies, including ours, 2DEG dominant Hall carrier densities are slightly increased with increasing temperature due to the thermal activation of bulk carriers at the barrier or other bulk-related layer [31,33,34]. After implementing QMSA method, 2DEG densities mostly show temperature independent behavior [22,26,33,35,36]. However, in this study, the 2DEG density extracted by QMSA is drastically decreased with increasing temperature. This is mainly because of the non-inclusion of a spacer layer that concludes a high level of interaction between 2DEG electrons and bulk electrons at the AlGaAs barrier. Theis et al. explained the interaction of the 2DEG electrons and bulk electrons with the trapping of DX-centers in the AlGaAs barrier layer as “*Trapping by DX centers reduces the*

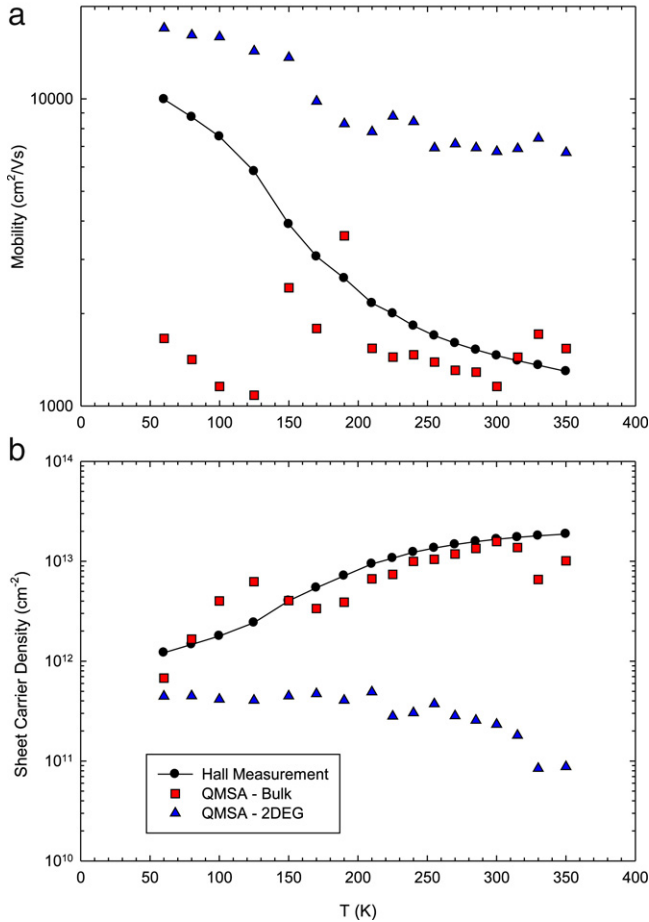


Fig. 2. Temperature dependent mobilities (a) and sheet carrier densities (b) of the carriers extracted by QMSA. Hall results are also shown for comparison.

net positive charge in the n-Al_xGa_{1-x}As. The overall charge neutrality is maintained as the density of free electrons in the GaAs conducting channel, and hence the channel conductivity is reduced" [3]. In our case, charge neutrality preservation shows itself with the reduction in the carrier density. Therefore, the electron transfer between the bulk and 2DEG channels at higher temperatures can be accepted as highly influenced by the DX-center trapping.

We solved the temperature dependent 1D Poisson–Schrödinger equations self-consistently in order to calculate the band structure and carrier density distribution without including the effects of DX-centers for the investigated heterostructure [37]. In Fig. 4, the temperature dependent carrier density distribution at the n-AlGaAs/GaAs interface is shown. Carrier density at the n-AlGaAs barrier layer is decreased and 2DEG density at the interface is increased with the decreasing temperature. These results are qualitatively matched with the experimental results. For the investigated samples, 2DEG is to be populated only at the first subband. The temperature dependent location of the first subband (ε_1) with respect to the Fermi level (ε_F) can be calculated from the well-know equation [38]

$$\varepsilon_F - \varepsilon_1 = \frac{kT}{e} \ln \left[\exp \left(\frac{n_{2DEG} e \pi \hbar^2}{m^* kT} \right) - 1 \right]. \quad (1)$$

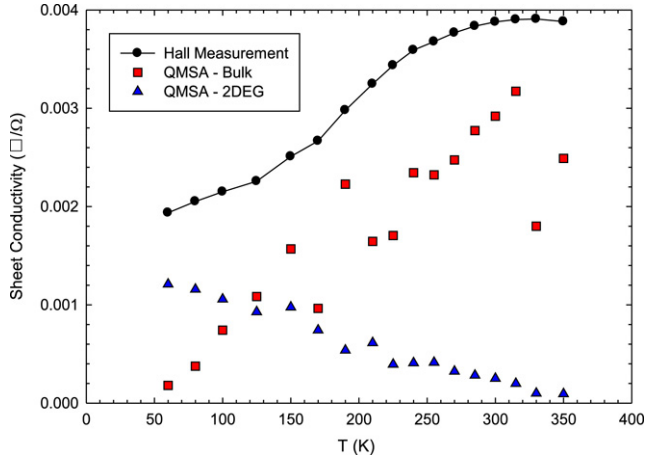


Fig. 3. Temperature dependent sheet conductivities calculated with Hall results and results extracted by QMSA.

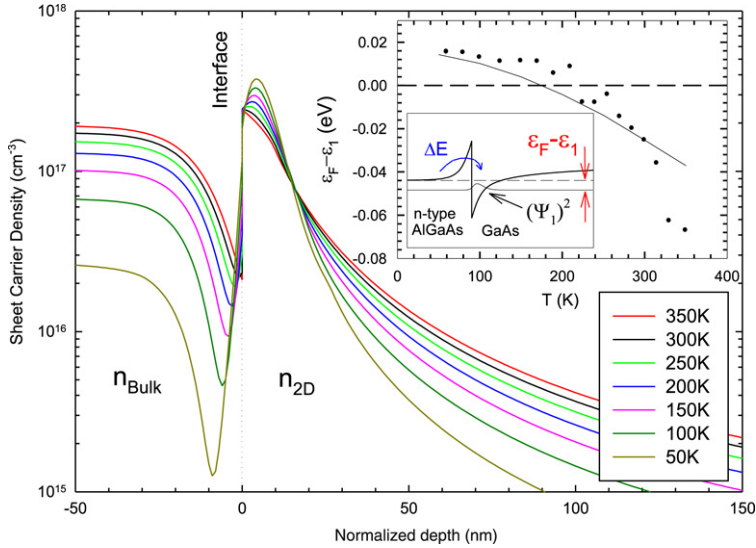


Fig. 4. Temperature dependent simulated carrier densities of n-AlGaAs barrier layer (n_{Bulk}) and the 2DEG (n_{2D}). Insert: Temperature dependent first subband energy with respect to the Fermi level for results extracted by QMSA results (filled circles) and results calculated with simulations (solid line). Conduction band diagram with Fermi level, effective barrier height (ΔE), first subband energy and the probability density of the 2DEG electron ($(\psi_1)^2$) is also shown in a box.

Here n_{2D} is the 2DEG carrier density and m^* is the effective mass. Eq. (1) is used to calculate first subband energy for measurement results extracted by QMSA (filled circles in the insert of Fig. 4) and for simulation results (solid line in the insert of Fig. 4). Because of the finite probability density of 2DEG at the barrier layer at low temperatures, the interface cannot be used as a separation point between the n_{2D} and bulk carrier density (n_{Bulk}). Therefore, these carrier density values are calculated with respect to the minimum carrier density point between these two populations (see Fig. 4). The results are in good agreement at low and mid-temperatures, which we can result in the 2DEG population being accepted as independent from DX-center influence. At higher temperatures, this agreement has become worse because of the n_{2D} diversity between the results extracted by QMSA and the simulation results.

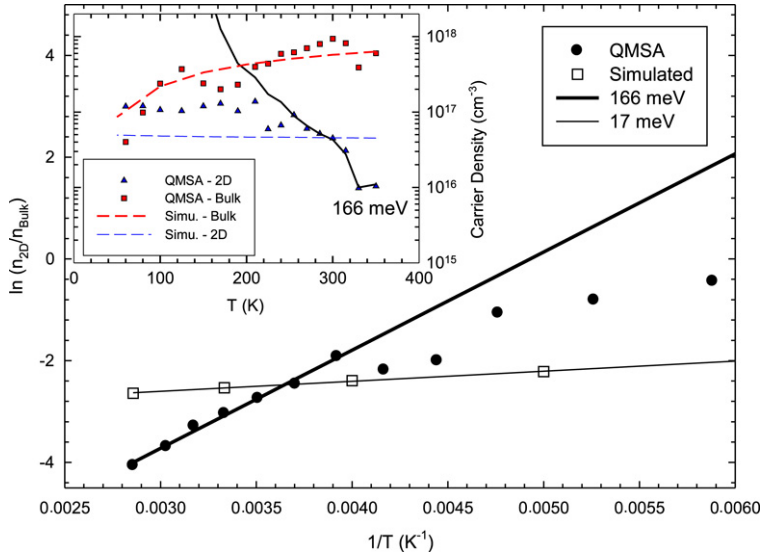


Fig. 5. Logarithm of the n_{2D}/n_{Bulk} as a function of the reciprocal temperature for the results extracted by QMSA and the simulation results. Fitted ΔE values are shown as full lines. Insert: Temperature dependent carrier densities of 2DEG carrier extracted by QMSA (blue triangles), bulk carrier extracted by QMSA (red squares), simulational 2DEG carrier (blue dashed line) and simulational bulk carrier (red dashed line). Full line shows the n_{2D} calculated with using $\Delta E = 166$ meV and n_{Bulk} values extracted by QMSA. (For interpretation of the references to colour in this figure legend, the reader is referred to the web version of this article.)

In Fig. 5 insert, n_{Bulk} and n_{2D} (red squares and blue triangles, respectively) values extracted by QMSA and the simulational values of n_{Bulk} and n_{2D} (red dashed line and blue dashed line, respectively) are shown. For the bulk carrier, the results extracted by QMSA and the simulation results are completely in agreement. For the 2D carrier, the averages of the results are in agreement. At low temperatures, the temperature dependence of both results that are extracted by QMSA and calculated with simulations show the same behavior. However, at temperatures above 200 K, the simulation values show more temperature independency.

The relation between n_{2D} and n_{Bulk} can be given with the equation

$$n_{2D} \propto n_{Bulk} e^{\Delta E/KT}. \quad (2)$$

Eq. (2) is a simple relationship to explain the real space charge transfer between quantum well (n_{2D}) and barrier layer (n_{Bulk}), and here ΔE is expected to be barrier discontinuity [39]. However, there is a dominant DX-center trapping in our case, and ΔE can be accepted as *effective barrier height*. Because of the effect of DX-centers at high temperatures [3], ΔE can be interpreted as the *DX-center activation energy*. Eq. (2) is used to calculate ΔE for the results extracted by QMSA and the results calculated with simulations. In Fig. 5, $\ln(n_{2D}/n_{Bulk})$ versus reciprocal temperature is shown. For the carrier densities that are calculated with simulation, the effective barrier height is found to be 17 meV, which is smaller than the barrier discontinuity value ($\Delta E = 113$ meV) for undoped $\text{Al}_{0.14}\text{Ga}_{0.86}\text{As}/\text{GaAs}$ [40]. For modulation doped $\text{AlGaAs}/\text{GaAs}$ heterostructures, the effective barrier height is expected to be low due to a tunneling possibility from the barrier to the quasitriangular well (see box in Fig. 4). For the carrier densities that are extracted by QMSA, ΔE is found to be 166 meV at high temperatures. At low temperatures, the value is converged to a simulation scale. The value of 166 meV is accepted as the DX-center activation energy of Si doping in the AlGaAs barrier layer, which is consistent with the literature values that are calculated by using the Hall data [6,19]. In Fig. 5 insert, full line shows n_{2D} values that calculated using Eq. (2) with $\Delta E = 166$ meV and n_{Bulk} values extracted by QMSA. As shown from the figure, high temperature behavior of n_{2D} can be explained successfully with Eq. (2) and active DX-center trapping.

4. Conclusion

Hall effect measurements on Si-doped $\text{Al}_{0.14}\text{Ga}_{0.86}\text{As}/\text{GaAs}$ heterostructures that are grown by MBE were carried out as a function of temperature (60–350 K) and as a function of a magnetic field (0–1.4 T). Magnetic field dependent Hall data are analyzed by using the quantitative mobility spectrum analysis (QMSA). With the QMSA, two conduction channels (2DEG at the $\text{AlGaAs}/\text{GaAs}$ interface and bulk electron at the barrier layer) were found over the studied temperature range. To explain the temperature dependent carrier density behaviors of these conducting channels, 1D self-consistent Schrödinger–Poisson equations were solved for the investigated samples. A high difference at high temperatures was observed for the 2DEG carrier density, in which this difference was explained with the DX-center trapping mechanism at the barrier layer. The barrier discontinuity value between the AlGaAs and GaAs layers was accepted as an effective barrier height. Moreover, because of the important DX-center influence at high temperatures ($T > 300$ K), an effective barrier height is accepted as DX-center activation energy. For the investigated samples, an effective barrier height value of 17 meV and a DX-center activation energy value of 166 meV are found by using simulations and results extracted by QMSA. The calculated DX-center activation energy value is in good agreement with the literature.

Acknowledgements

This work is supported by the State Planning Organization of Turkey under Grant No. 2001K120590 and by the European Union under the projects EU-PHOME, and EU-ECONAM, and TUBITAK under Project Numbers 105A005, 106E198, and 107A004. One of the authors (E.O.) also acknowledges partial support from the Turkish Academy of Sciences.

References

- [1] P.M. Mooney, P.M. Solomon, T.N. Theis, in: B. de Cremoux (Ed.), 11th Int. Symp. On Gallium Arsenide and Related Compounds, Biarritz, France, 1984, Adam Hilger, Bristol, 1985, p. 617.
- [2] K.R. Hoffman, E. Kohn, *Electron. Lett.* 22 (1986) 335.
- [3] T.N. Theis, B.D. Parker, P.M. Solomon, S.L. Wright, *Appl. Phys. Lett.* 49 (1986) 1542.
- [4] R. Fischer, T.J. Drummond, J. Klem, W. Kopp, T.S. Henderson, D. Perrachione, H. Morkoc, *IEEE Trans. Electron Devices* 31 (1984) 1028.
- [5] D.V. Lang, R.A. Logan, M. Jaros, *Phys. Rev. B* 19 (1979) 1015.
- [6] D.V. Lang, in: S.T. Pantelides (Ed.), *Deep Centers in Semiconductors*, Gordon and Breach Science Publishers, New York, 1986, p. 489.
- [7] M. Mizuta, M. Tachikawa, H. Kukimoto, S. Minimura, *Japan. J. Appl. Phys.* 24 (1985) L143.
- [8] M.F. Li, P.Y. Yu, E.R. Weber, W. Hansen, *Appl. Phys. Lett.* 51 (1987) 349.
- [9] P.M. Mooney, *J. Appl. Phys.* 67 (1990) R1.
- [10] S.B. Zhang, S.-H. Wei, A. Zunger, *Phys. Rev. Lett.* 84 (2000) 1232.
- [11] S.-H. Wei, S.B. Zhang, *Phys. Rev. B* 66 (2002) 155211.
- [12] J. Li, S.-H. Wei, L.-W. Wang, *Phys. Rev. Lett.* 94 (2005) 185501.
- [13] O. Kumagai, H. Kawai, Y. Mori, K. Kaneko, *Appl. Phys. Lett.* 45 (1984) 1322.
- [14] M. Tachikawa, M. Mizuta, H. Kukimoto, *Japan. J. Appl. Phys.* 23 (1984) 159.
- [15] R.J. Nelson, *Appl. Phys. Lett.* 31 (1977) 351.
- [16] J.J. Yang, L.A. Moudy, W.I. Simpson, *Appl. Phys. Lett.* 40 (1982) 244.
- [17] K. Kaneko, M. Ayabe, N. Watanabe, in: C. Hilsun (Ed.), *Gallium Arsenide and Related Compounds*, Edinburgh, 1976, IOP, Bristol, 1977, p. 216.
- [18] M.O. Watanabe, K. Morizuka, M. Mashita, Y. Ashizawa, Y. Zohta, *Japan. J. Appl. Phys.* 23 (1984) L103.
- [19] E.F. Schubert, K. Ploog, *Phys. Rev. B* 30 (1984) 7021.
- [20] T. Ishikawa, T. Yamamoto, K. Kondo, *Japan. J. Appl. Phys.* 25 (1986) L484.
- [21] H.L. Störmer, A.C. Gossard, W. Wiegmann, K. Baldwin, *Appl. Phys. Lett.* 39 (1981) 912.
- [22] S.B. Lisesivdin, S. Demirezen, M.D. Caliskan, A. Yildiz, M. Kasap, S. Ozelcik, E. Ozbay, *Semicond. Sci. Technol.* 23 (2008) 095008.
- [23] J. Antoszewski, D.J. Seymour, L. Faraone, J.R. Meyer, C.A. Hoffman, *J. Electron. Mater.* 24 (1995) 1255.
- [24] J.R. Meyer, C.A. Hoffman, J. Antoszewski, L. Faraone, *J. Appl. Phys.* 81 (1997) 709.
- [25] B.C. Dodrill, J.R. Lindemuth, B.J. Kelley, G. Du, J.R. Meyer, *Compound Semicond.* 7 (2001) 58.
- [26] N. Biyikli, J. Xie, Y.T. Moon, F. Yun, C.G. Stefanita, S. Bandyopadhyay, H. Morkoc, I. Vurgaftman, J.R. Meyer, *Appl. Phys. Lett.* 88 (2006) 142106.
- [27] J.S. Kim, D.G. Seiler, W.F. Tseng, *J. Appl. Phys.* 73 (1993) 8324.
- [28] M.J. Kane, N. Apsley, D.A. Anderson, L.L. Taylor, T. Kerr, *J. Phys. C: Solid State Phys.* 18 (1985) 5629.
- [29] M.C. Gold, D.A. Nelson, *J. Vac. Sci. Technol. A* 4 (1986) 2040.

- [30] W.A. Beck, J.R. Anderson, *J. Appl. Phys.* 62 (1987) 541.
- [31] S.B. Lisesivdin, A. Yildiz, S. Acar, M. Kasap, S. Ozelik, E. Ozbay, *Appl. Phys. Lett.* 91 (2007) 102113.
- [32] I. Vurgaftman, J.R. Meyer, C.A. Hoffman, D. Redfern, J. Antoszewski, L. Faraone, J.R. Lindemuth, *J. Appl. Phys.* 84 (1998) 4966.
- [33] S.B. Lisesivdin, S. Acar, M. Kasap, S. Ozelik, S. Gokden, E. Ozbay, *Semicond. Sci. Technol.* 22 (2007) 543.
- [34] S. Gokden, *Phys. Status Solidi (a)* 2 (2003) 369.
- [35] Z. Dziuba, J. Antoszewski, J.M. Dell, L. Faraone, P. Kozodoy, S. Keller, B. Keller, S.P. Denbaars, U.K. Mishra, *J. Appl. Phys.* 82 (1997) 2996.
- [36] J. Antoszewski, L. Faraone, *Opto-Electron. Rev.* 12 (2004) 347.
- [37] S. Birner, S. Hackenbuchner, M. Sabathil, G. Zandler, J.A. Majewski, T. Andlauer, T. Zibold, R. Morschl, A. Trellaki, P. Vogl, *Acta Phys. Polon. A* 110 (2006) 111.
- [38] J. Singh, *Semiconductor Optoelectronics: Physics and Technology*, McGraw-Hill, New York, 1995, p. 125.
- [39] J. Singh, *Physics of Semiconductors and Their Heterostructures*, McGraw-Hill, New York, 1993, p. 519.
- [40] A.J. Hill, P.H. Ladbrooke, *Electron. Lett.* 22 (1986) 218.